JACS
JOURNAL OF THE AMERICAN CHEMICAL SOCIETY
Article
pubs.acs.org/JACS

All-Benzene Carbon Nanocages: Size-Selective Synthesis, Photophysical Properties, and Crystal Structure

Katsuma Matsui,[†] Yasutomo Segawa,*[,†,‡] and Kenichiro Itami*[,†,‡,§]

[†]Graduate School of Science, Nagoya University, Japan, Chikusa, Nagoya 464-8602, Japan
[‡]JST ERATO, Itami Molecular Nanocarbon Project, Nagoya University, Chikusa, Nagoya 464-8602, Japan
[§]Institute of Transformative Bio-Molecules (WPI-ITbM), Nagoya University, Chikusa, Nagoya 464-8602, Japan

Supporting Information

ABSTRACT: The design and synthesis of a series of carbon nanocages consisting solely of benzene rings are described. Carbon nanocages are appealing molecules not only because they represent junction unit structures of branched carbon nanotubes, but also because of their potential utilities as unique optoelectronic π-conjugated materials and guest-encapsulating hosts. Three sizes of strained, conjugated [*n.n.n*]carbon nanocages (**1**, $n = 4$; **2**, $n = 5$; **3**, $n = 6$) were synthesized with perfect size-selectivity. Cyclohexane-containing units and 1,3,5-trisubstituted benzene-containing units were assembled to yield the minimally strained bicyclic precursors, which were successfully converted into the corresponding carbon nanocages via acid-mediated aromatization. X-ray crystallography of **1** confirmed the cage-shaped structure with an approximately spherical void inside the cage molecule. The present studies revealed the unique properties of carbon nanocages, including strain energies, size-dependent absorption and fluorescence, as well as unique size-dependency for the electronic features of **1**−**3**.

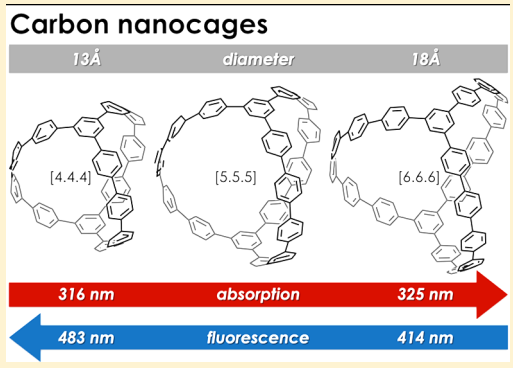

INTRODUCTION

Carbon nanotube (CNT) segments and molecular nanocarbons have captivated the attention of the broad scientific community from both fundamental and application perspectives.[1] For example, there is an enormous expectation for CNT segment molecules to serve as templates for structurally uniform CNTs.[2] In addition, due to their unique arrangement of π-systems, CNT segment molecules are extremely interesting functional small molecules in its own right. However, due to the general difficulty in building up significant strain energy during their synthesis and to the lack of appropriate strategies and component-assembling reactions, it was only until recently that the chemistry of CNT segment molecules expanded rapidly.[1−3]

One of the most featured CNT segment molecules in recent years are cycloparaphenylenes (CPPs),[3] which are ring-shaped molecules that correspond to the shortest sidewall segment of armchair CNTs (Figure 1). Since the first successful synthesis of CPP by Bertozzi and Jasti in 2008,[4] the groups of Itami, Jasti, Yamago, Isobe, Müllen, Wegner, and Wang reported the synthesis of various sizes of [*n*]CPPs ($n = 5$−16, 18),[5−7] functionalized CPPs,[8−10] and CPP-related carbon nanorings.[11−13] In 2013, our group finally showed that CNTs can be synthesized in a diameter-selective fashion by using CPPs as templates.[14] In addition to being used as carbon nanotube templates, CPPs themselves are useful functional molecules. Representative interesting properties of CPPs include the size-dependent photophysical properties[15] and their host−guest ability.[16]

In 2012, we designed and proposed all-benzene carbon nanocages, three-dimensional cage-shaped conjugated hydrocarbons consisting solely of sp^2-carbons and covalent bonds, as a new family of molecular nanocarbons (Figure 1).[17] The [*n.n.n*]carbon nanocages consist of three [*n*]paraphenylene bridges connected by two benzene-1,3,5-triyl bridgeheads. As carbon nanocages represent junction units of branched CNTs (Figure 1), the conditions we developed for CPP-to-CNT (ring-to-tube) conversion could be applied for the bottom-up synthesis of branched CNTs using carbon nanocages as templates. Moreover, carbon nanocages should have vast utility in host−guest chemistry as well as in the field of organic electronics.[18]

We herein report the size-selective synthesis of [4.4.4]carbon nanocage (**1**) and [5.5.5]carbon nanocage (**2**), adding to [6.6.6]carbon nanocage (**3**), which we previously reported.[17] With these carbon nanocages of different sizes in hand, it was possible to uncover the size effect in photophysical properties. In addition, the first X-ray crystal structure of carbon nanocage (**1**) is reported. It should be noted that, Yamago recently disclosed another class of carbon nanocages, which display interesting properties.[19]

Received: September 25, 2014
Published: October 31, 2014

ACS Publications © 2014 American Chemical Society

dx.doi.org/10.1021/ja509880v | J. Am. Chem. Soc. 2014, 136, 16452−16458

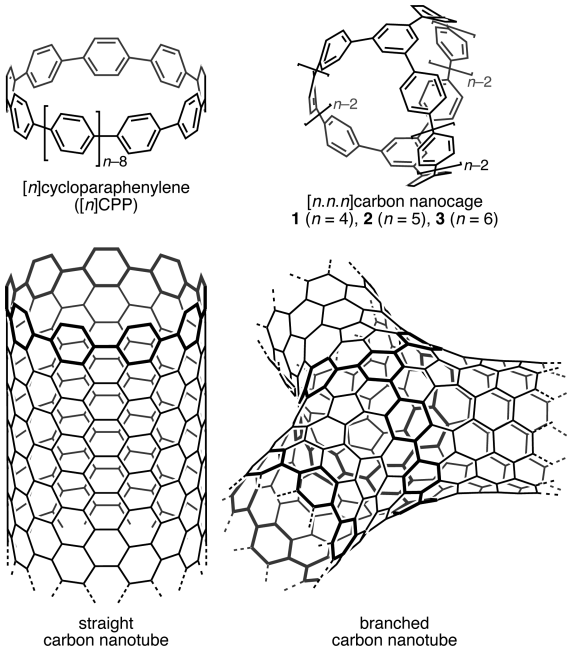

Figure 1. [*n*]Cycloparaphenylene ([*n*]CPP) and [*n.n.n*]carbon nanocages (**1**–**3**) as segments of straight and branched carbon nanotubes.

RESULT AND DISCUSSION

1. Structural Features of Carbon Nanocages Investigated by DFT Calculation. To gain insight into the structural features of carbon nanocages, DFT calculations of **1**–**3** were conducted by Gaussian09 program with the B3LYP/6-31G(d) level of theory. Optimized structures of **1**–**3** are shown in Figure 2. Symmetries of the optimized structures are D_3 (**1**, **3**) and C_{3h} (**2**), the difference of which comes from the even or odd number of bridged phenylene rings. The cages contain approximately spherical voids. The distances between the two trisubstituted benzene rings of **1**, **2**, and **3** are 13.0, 15.8, and 18.4 Å, respectively, and their radii estimated from the top view are 7.2, 8.5, and 10.1 Å, respectively, as shown in Figure 2. The sizes of the [*n.n.n*]carbon nanocages are in between those of the corresponding [2*n* + 1]CPP and [2*n* + 2]CPP.[15a]

On the basis of hypothetical homodesmotic reactions, we estimated the strain energies (SE) for **1**–**3** to be 96.0, 80.0, and 67.2 kcal·mol^{-1}, respectively (see the Supporting Information for details). Although these values are comparable to those of very small CPPs (e.g. $SE_{[6]CPP}$ = 96.0 kcal·mol^{-1}),[11a] the real stain on the cage molecules should be estimated by the strain energies per carbon atom. Thus, the strain energies for **1**–**3** and [6]–[16]CPP per carbon atom versus diameter are plotted in Figure 3, showing that the carbon nanocages share the same class of strained macrocycles with CPP.[20] These results indicate that similar sizes of carbon nanocages and CPPs are almost equally strained, and we thus envisioned that the synthetic strategy for middle-size CPPs should be applicable to the synthesis of these carbon nanocages.

2. Synthesis of Carbon Nanocages. *2-1. Strategy and Overview.* The methodology we have developed for CPP synthesis uses cyclohexane moieties as bent benzene precursors. The combination of *cis*-diphenylcyclohexane and phenylene diboronic acid produced strain-free macrocycles, which could then be transformed to the corresponding [9]–[16]CPPs (Figure 4, eq 1).[5a–e] For the synthesis of smaller CPPs such as

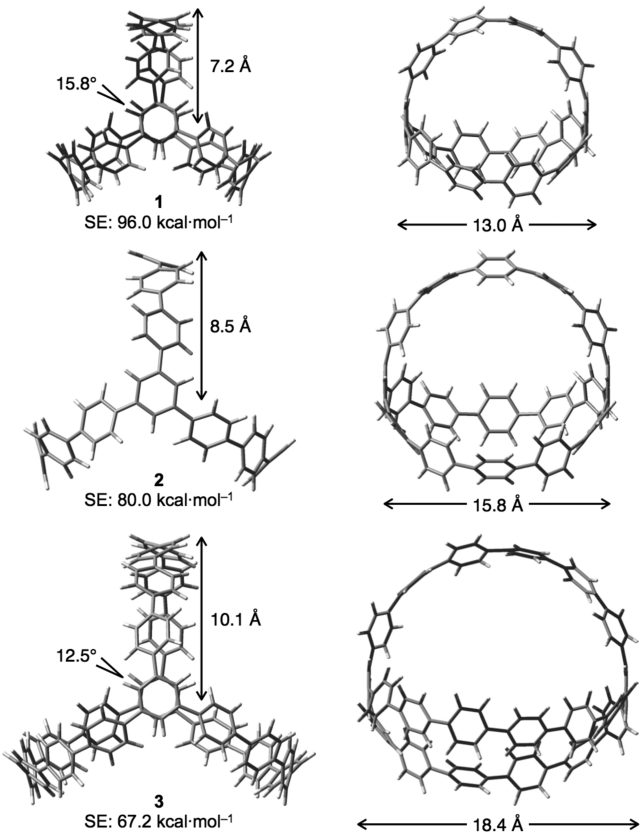

Figure 2. Optimized structures of carbon nanocages **1**–**3** from top (left) and side (right) view with strain energies (SE).

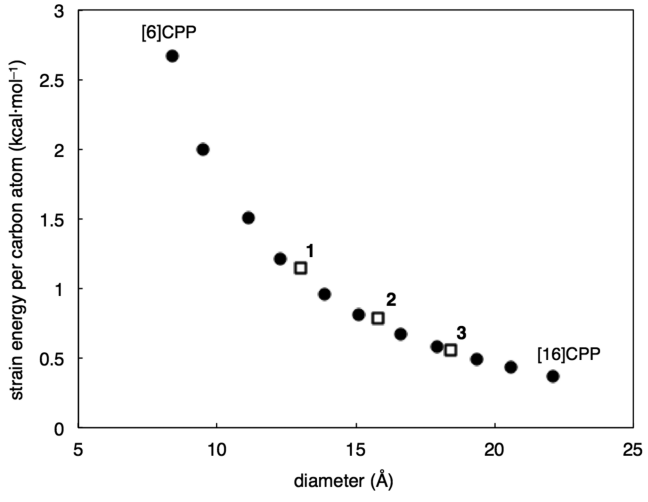

Figure 3. Strain energies of carbon nanocages **1**–**3** (square) and [6]–[16]CPP (filled circle) per carbon atom versus diameters (B3LYP/6-31G(d)).

[7] and [8]CPP, the phenylcyclohexanone derivative was employed to form triangular macrocycles (eq 2).[5f]

Meanwhile, for the synthesis of carbon nanocages, the route was designed so that unstrained bicyclic precursors could be synthesized by the combination of cyclohexane-containing units and trisubstituted benzene units instead of the paraphenylene unit (eq 3). Through this synthetic route, [6.6.6]carbon nanocage (**3**) was successfully synthesized.[17] To synthesize smaller carbon nanorings (**1** and **2**), a phenylcyclohexanone derivative was chosen for the small bent unit (eq 4).

dx.doi.org/10.1021/ja509880v | J. Am. Chem. Soc. 2014, 136, 16452–16458

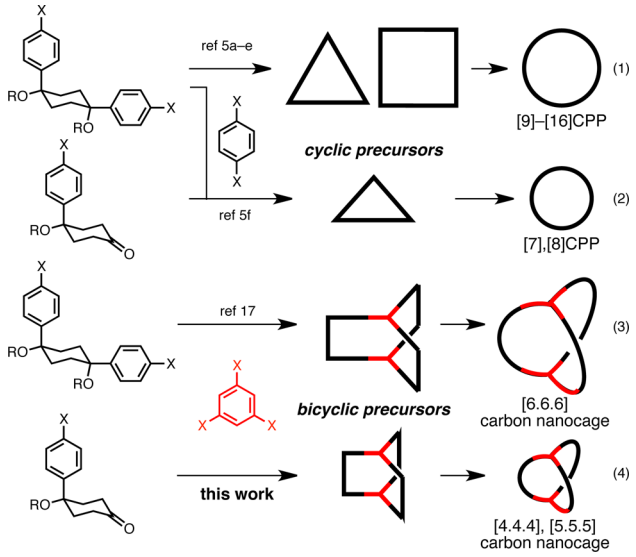

Figure 4. Outline of synthesis of [*n*]cycloparaphenylenes and [*n.n.n*]carbon nanocages. X = halogen or boryl group. R = H or methoxymethyl.

*2-2. Synthesis of [6.6.6]Carbon Nanocage (**3**).* Scheme 1 outlines the synthesis of [6.6.6]carbon nanocage (**3**). The

Scheme 1. Synthesis of Carbon Nanocage 3

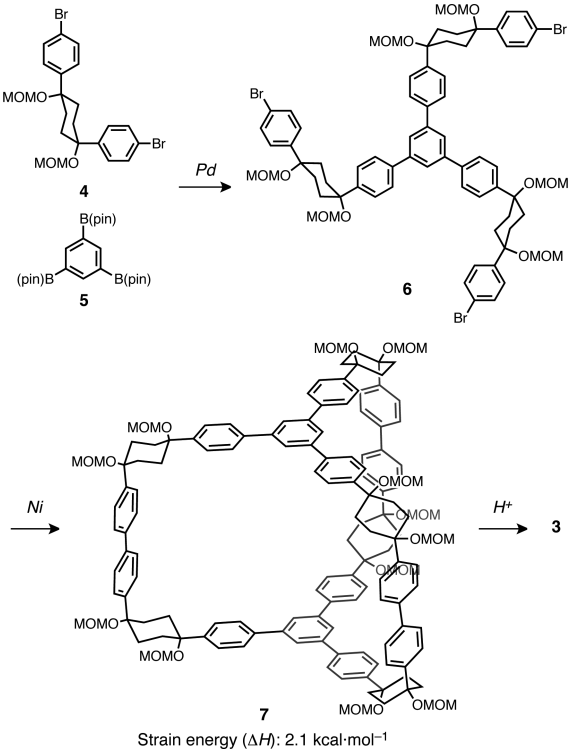

palladium-catalyzed Suzuki–Miyaura coupling reaction between L-shaped unit **4** and 1,3,5-triborylbenzene **5** provided a trifurcated unit **6**, a molecule with C_3 symmetry. Compound **6** was then subjected to a 3-fold homocoupling reaction mediated by Ni(cod)$_2$/2,2′-bipyridyl (cod = 1,5-cyclooctadiene) to produce bicyclic macrocycle **7**. Treatment of **7** with acid afforded [6.6.6]carbon nanocage (**3**) through conversion of the cyclohexane moieties to benzene rings.[17]

*2-3. Synthesis of [4.4.4]Carbon Nanocage (**1**) and [5.5.5] Carbon Nanocage (**2**).* For the synthesis of smaller carbon nanocages **1** and **2**, small bicyclic macrocycles, shown in Scheme 2, were designed as possible precursors for these cages.

Scheme 2. Retrosynthesis of Carbon Nanocages 1 and 2

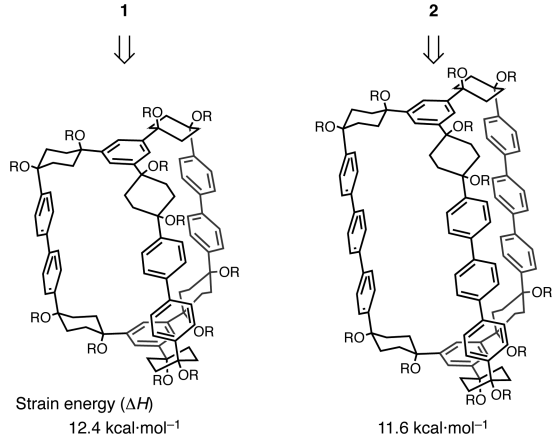

These macrocyclic precursors differ from **7** in that the three cyclohexane moieties are directly attached to the central trisubstituted benzene rings. The strain energies of the precursors for **1** and **2** are 12.4 and 11.6 kcal·mol^{-1}, respectively, which are greater than the 2.1 kcal·mol^{-1} value found for **7** (see the Supporting Information for details). Those molecules are more strained compared to **7** probably due to the steric hindrance at the 1,3,5-tricyclohexylbenzene moieties.

On the basis of these considerations, [4.4.4]carbon nanocage (**1**) and [5.5.5]carbon nanocage (**2**) were synthesized as follows. The requisite trifurcate unit was synthesized from a new cyclohexane unit, 4-(4-chlorophenyl)-4-hydroxycyclohexan-1-one (**9**), which can be prepared from 1-bromo-4-chlorobenzene and 1,4-cyclohexanedione monoethyleneketal in three steps.[5f] Thus, 3,5-dibromophenyllithium, generated by the lithiation of 1,3,5-tribromobenzene (**8**) with *n*-BuLi, was reacted with **9** to provide **10**. The crude mixture was subjected to methoxymethyl (MOM) protection to afford *cis* compound **11** in 60% yield after two steps. The corresponding *trans* isomer was also formed, but this could be easily separated from **11** by silica-gel column chromatography. Subjecting **11** to an identical reaction sequence (lithiation, carbonyl addition, MOM protection) provided the two-arm compound **13** in moderate yield. After isolation, **13** was then subjected to a similar sequence, yielding the trifurcated framework **14** in 72% yield. Finally, MOM protection of **14** proceeded smoothly to yield **15** in 94% yield. The trifurcated and fully *cis* structure of **15** was unambiguously confirmed by X-ray crystallography (Scheme 3), the single crystal for which was obtained from hot 2-propanol solution. Then, the Miyaura borylation of **15** was conducted with the Pd$_2$(dba)$_3$/X-Phos catalyst to yield **16**, a viable coupling partner, in 93% yield. To synthesize nanocage **2**, a one-benzene extended coupling unit **17** was prepared by the Suzuki–Miyaura coupling of triborylated compound **16** and 1,4-dibromobenzene in the presence of PdCl$_2$(dppf) catalyst and Ag$_2$O (62% yield).

Synthesis of the bicyclic precursors and carbon nanorings **1** and **2** is shown in Scheme 4. Bicyclic macrocycle **18**, the primary precursor of **1**, was synthesized in 9% yield by the 3-fold homocoupling of **15** mediated by Ni(cod)$_2$/1,10-

dx.doi.org/10.1021/ja509880v | J. Am. Chem. Soc. 2014, 136, 16452–16458

Scheme 3. Preparation of Trifurcate Units[a]

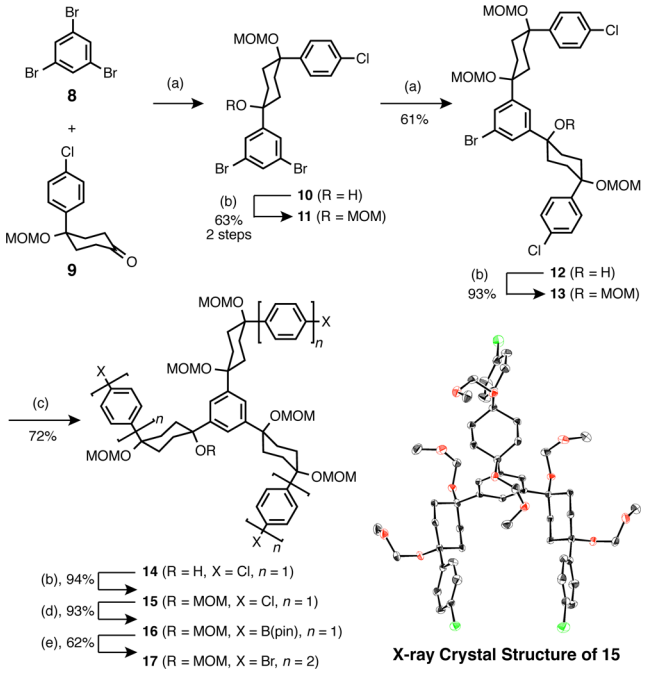

[a]Reaction conditions: (a) bromide (**8** or **11**), *n*-BuLi, Et_2O, −78 °C; then **9**. (b) $^iPr_2NEt$, MOMCl, CH_2Cl_2, rt. (c) *n*-BuLi, Et_2O/THF = 2:1, −78 °C; then **9**. (d) $B_2(pin)_2$, $Pd_2(dba)_3$, X-Phos, KOAc, 1,4-dioxane, 110 °C. (e) 1,4-dibromobenzene, $PdCl_2(dppf)$, K_2CO_3, Ag_2O, toluene/water, 80 °C. MOM = methoxymethyl, B(pin) = 4,4,5,5-tetramethyl-1,3,2-dioxaborolan-2-yl, X-Phos =2-dicyclohexylphosphino-2′,4′,6′-triisopropylbiphenyl, dppf = 1,1′-diphenylphosphinoferrocene.

Scheme 4. Synthesis of Carbon Nanocages 1 and 2[a]

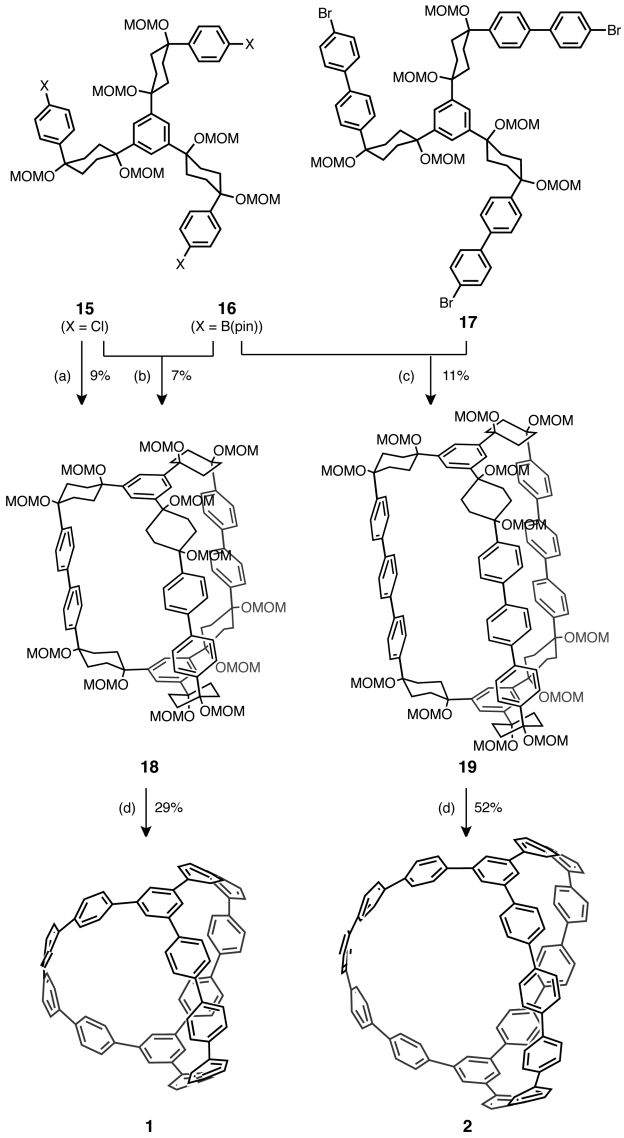

[a]Reaction conditions: (a) $Ni(cod)_2$, 1,10-phenanthroline, THF, reflux. (b) $Pd(OAc)_2$, S-Phos, K_3PO_4, 1,4-dioxane/water, 100 °C. (c) $PdCl_2(dppf)$, K_2CO_3, toluene/water, 80 °C. (d) $NaHSO_4{\cdot}H_2O$, *o*-chloranil, *m*-xylene/DMSO, 150 °C. S-Phos = 2-dicyclohexylphosphino-2′,6′-dimethoxybiphenyl.

phenanthrolin. Compound **18** could also be prepared by a palladium-catalyzed cross-coupling of **15** and its boronate counterpart **16**, albeit in somewhat lower yield (7%). Palladium-catalyzed cross-coupling reaction between **16** and **17** produced a larger bicyclic macrocycle **19** in 11% yield. The final cyclohexane-to-benzene transformation (aromatization) was achieved by treatment of **18** and **19** with $NaHSO_4{\cdot}H_2O$ and *o*-chloranil in *m*-xylene/DMSO under reflux conditions, furnishing [4.4.4]carbon nanocage (**1**) and [5.5.5]carbon nanocage (**2**) in 29% and 53% yield, respectively. The formation of these nanocages was confirmed by ^1H and ^{13}C NMR spectroscopy, HH COSY, HMQC, and high-resolution MALDI-TOF mass spectrometry. It is worth noting that the ^1H NMR chemical shifts for the singlet on the 1,3,5-benzenetriyl moieties of **1**, **2**, and **3** are 7.65, 7.79, and 7.85 ppm, respectively, showing a downfield shift with an increase in size; the same tendency as observed in CPPs.[4−7]

3. X-ray Crystal Structure of Carbon Nanocage 1. The cage-shaped structure of [4.4.4]carbon nanocage (**1**) was unambiguously confirmed by X-ray crystallography (Figure 5). A single crystal was obtained from a THF solution of **1** through slow addition of Et_2O vapor at room temperature. THF and Et_2O molecules were observed within the crystal structure for every cage molecule with disordering. The shape of **1** was slightly distorted in the solid state with respect to the calculated structure; the cavity inside became ellipsoidal rather than spherical (see the Supporting Information for details). Figure 6 shows the packing modes of **1** in the *bc* plane and *ac* plane. These figures clearly show that nanocage **1** packs tightly, with paraphenylene bridges filling the grooves of adjacent molecules. Similar to CPPs, no significant $\pi-\pi$ interaction was observed in the solid state of **1**, most likely because the walls of cage **1** are bent (convex-to-convex π-stacking is unfavorable). Furthermore, Figure 6b shows the presence of a linear void channel, suggesting that **1** may be useful as gas-storage material if solvent-free crystals of **1** could be obtained.

4. Cyclic Voltammetry of Carbon Nanocages. The cyclic voltammetry of carbon nanocages **1**−**3** was next measured. The cyclic voltammograms are shown in Figure 7 along with the oxidation potentials E_{ox}. The values of E_{ox} are determined from the center voltage between the peak for the oxidation of the sample and the peak for the reduction of the oxidized sample. All the carbon nanocages showed reversible oxidation waves indicative of the stability of the cationic species generated in these cage skeletons. The first oxidation potential increases as the number of paraphenylene units increases.

dx.doi.org/10.1021/ja509880v | J. Am. Chem. Soc. 2014, 136, 16452−16458

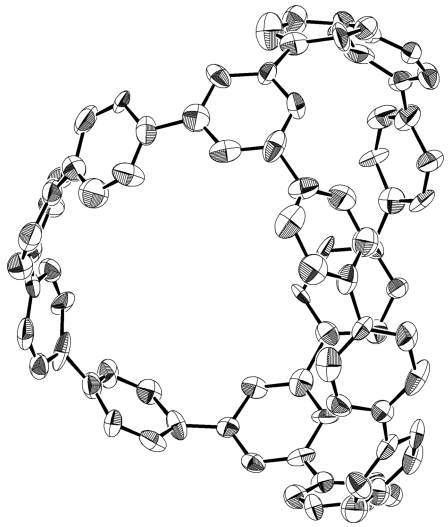

Figure 5. ORTEP drawing of **1**·THF·Et_2O with 50% thermal ellipsoids. All hydrogen atoms, THF and Et_2O molecules are omitted for clarity.

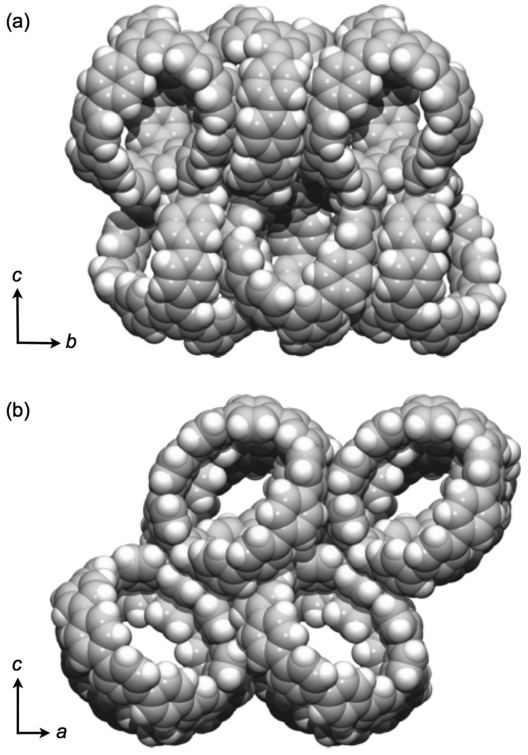

Figure 6. Packing structures of **1**. (a) *bc* plane, (b) *ac* plane.

5. Photophysical Properties of Carbon Nanocages. The photophysical properties (UV−vis absorption and fluorescence) of carbon nanocages **1**−**3** were also investigated (Figure 8); the results are summarized in Table 1. Absorption maxima (λ_{abs}) were observed at 316, 321, and 325 nm for **1**, **2**, and **3**, respectively, with molecular absorption coefficients (ε) of 9.4×10^4, 1.8×10^5, and 1.9×10^5 cm^{-1} M^{-1}, respectively. The broadness of the spectra (380−420 nm) may imply the existence of weak absorption peaks. The absorption wavelengths of **1**−**3** are red-shifted with increasing cage sizes. This trend is in sharp contrast to that of CPPs where they all exhibit absorption maxima at 338−339 nm regardless of their ring sizes.[15] On the other hand, the fluorescence maxima, determined by the negative second derivatives (see the Supporting Information for details), are gradually blue-shifted as the cage size increases. This tendency is the same as the case of CPPs. All carbon nanocages exhibit intense blue fluorescence with high fluorescence quantum yields (Φ_F = 0.66 (**1**), 0.76 (**2**), 0.87 (**3**)) as shown in Figure 8b.

To shed light on the nature of the electrochemical and photophysical properties of the carbon nanocages, time-dependent DFT (TD-DFT) calculations of the optimized structures of **1**−**3** at the same calculation level (B3LYP/6-31G(d)) were performed. In line with CV measurement, the smaller cage has higher HOMO energy levels. Forbidden transitions at the highest wavelength regions (377 nm (**1**), 372 nm (**2**), 371 nm (**3**)) were found as HOMO/HOMO − 1 → LUMO/LUMO + 1 transitions in which the pairs of HOMO/

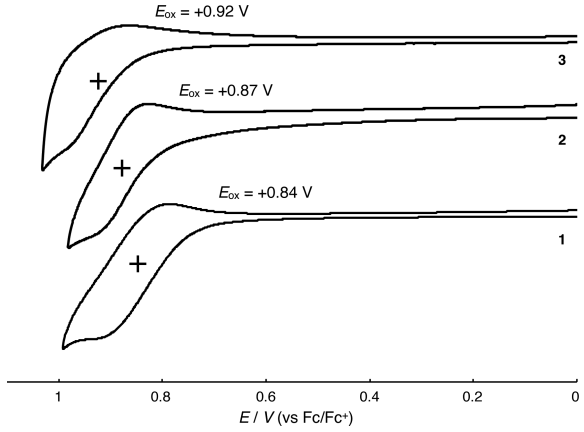

Figure 7. Cyclic voltammograms of **1**−**3** in *n*-Bu_4NPF_6/CH_2Cl_2 at room temperature.

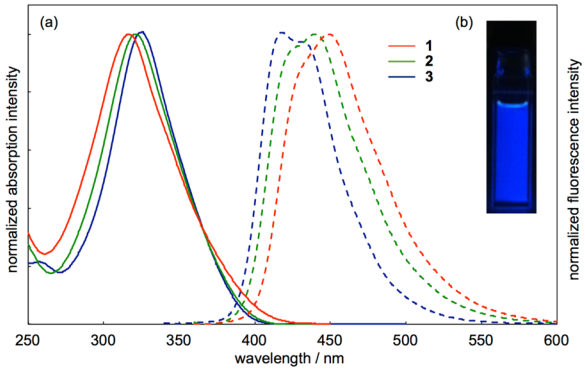

Figure 8. (a) UV−vis absorption (solid line) and fluorescence (broken line) spectra of **1** (red), **2** (green), and **3** (blue) in chloroform. (b) Fluorescence of chloroform solution of **1**.

Table 1. Photophysical Data for [*n.n.n*]Carbon Nanocages[a]

	absorption	fluorescence	
compound	λ_{abs} [nm][b]	λ_{em} [nm][c]	Φ_F[d]
1	316	427, 454, 483	0.66
2	321	418, 445, 476	0.76
3	325	414, 439, 471	0.87

[a]In chloroform. [b]The highest absorption maxima are given. [c]Emission maxima determined by negative second derivative are given. [d]Absolute fluorescence quantum yields determined by a calibrated integrating sphere system within ±3%.

dx.doi.org/10.1021/ja509880v | J. Am. Chem. Soc. 2014, 136, 16452−16458

HOMO − 1 and LUMO/LUMO + 1 are degenerated. Complicated transitions including 10 orbitals from HOMO − 4 to LUMO + 4 were found at around 330 nm. It can be explained that the blue-shift of shoulder peaks in absorption and fluorescence maxima is due to increasing of the HOMO−LUMO gap[21] as the size of the nanocage increases, as shown in Figure 9a.

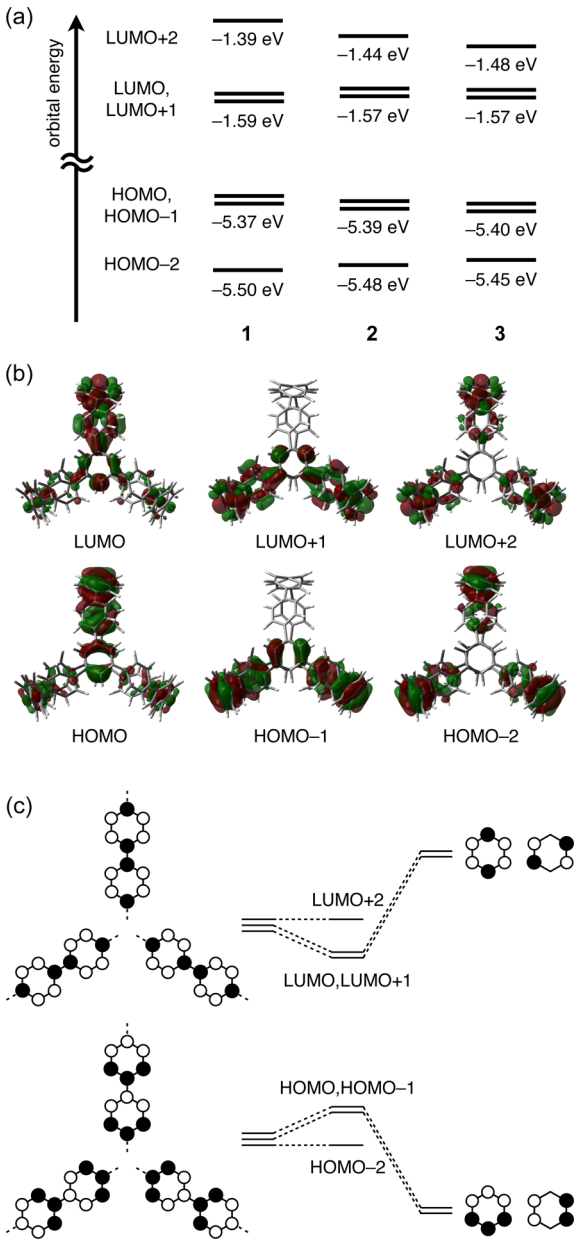

Figure 9. (a) Energy diagrams of the frontier MOs of **1**−**3**. (b) Pictorial representations of the frontier MOs of **1** calculated at the B3LYP/6-31G(d) level of theory. (c) Components of frontier MOs of **1**−**3**.

We then questioned why the HOMO−LUMO gap increases as the size of nanocage increases. In the case of CPPs, where the same tendency is observed, we explained that the bending effect is the main contributor to the HOMO−LUMO gap.[15b] Careful investigation of the frontier orbitals of carbon nanocages provides us different reasons. Depicted in Figure 9b are six representative frontier orbitals of **1**. These orbitals are the combination of the orbitals of three independent paraphenylenes and two bridgehead benzene rings as shown in Figure 9c. Because two orbitals are degenerate at the HOMO of benzene, two orbitals (HOMO and HOMO − 1) are created by two of the three paraphenylene orbitals and two benzene orbitals. The other HOMO of paraphenylene remains as HOMO − 2 of the cage. The energy of HOMO − 2 is raised as the size of the nanocage increases, because the length of paraphenylene is the main contributor in this case. The energy difference between HOMO − 2 and HOMO/HOMO − 1 reflects the degree of interaction between paraphenylenes and central benzene rings, which is probably affected by dihedral angles of the central benzene and connecting phenylene (25.2° (**1**), 25.7° (**2**), 29.3° (**3**)). The energy levels of unoccupied orbitals (LUMO, LUMO + 1, and LUMO + 2) can also be explained in a similar manner. We conclude that the characteristic blue-shift of the absorption and fluorescence spectra of [*n.n.n*]carbon nanocages comes from the orbital interactions between three [*n*]paraphenylene bridges with two benzene bridgeheads.

CONCLUSION

In summary, three sizes of strained, conjugated carbon nanocages consisting solely of covalently bound benzene rings were synthesized. Cyclohexane-containing units and 1,3,5-trisubstituted benzene-containing units were assembled through stepwise addition to yield the minimally strained bicyclic precursors, which were in turn successfully converted into the corresponding carbon nanocages via acid-mediated aromatization. X-ray crystallography of **1** confirmed the cage-shaped structure with an approximately spherical void. Electrochemical and photophysical measurements and DFT studies revealed the unique properties of carbon nanocages, including strain energies, size-dependent absorption and fluorescence spectra, and degeneration of HOMO/HOMO − 1 and LUMO/LUMO + 1. With three sizes of carbon nanocages in hand, further investigations are underway in our laboratory, including determination of the guest-encapsulating properties of carbon nanocages and the possibility of bottom-up chemical synthesis of branched carbon nanotubes using these unique molecules.

ASSOCIATED CONTENT

Supporting Information

Experimental procedures, spectra of new compounds, and details of computational studies. CCDC 1006531 (**1**·THF·Et_2O), 1006666 (**15**). This material is available free of charge via the Internet at http://pubs.acs.org.

AUTHOR INFORMATION

Corresponding Authors

ysegawa@nagoya-u.jp
itami@chem.nagoya-u.ac.jp

Notes

The authors declare no competing financial interest.

ACKNOWLEDGMENTS

This work was supported by the ERATO program from JST (K.I.) and the Funding Program for Next Generation World-Leading Researchers from JSPS (K.I.). K.M. is a recipient of JSPS fellowship for young scientists. We thank Dr. Hiroshi Ueno (Nagoya Univ.) for assistance of cyclic voltammetry, and

Dr. Ayako Miyazaki (Nagoya Univ.) for fruitful discussion and critical comments. Calculations were performed using the resources of the Research Center for Computational Science, Okazaki, Japan. ITbM is supported by the World Premier International Research Center (WPI) Initiative, Japan.

REFERENCES

(1) Bunz, U. H. F.; Menning, S.; Martin, N. *Angew. Chem., Int. Ed.* **2012**, *51*, 7094.

(2) (a) Fort, E. H.; Donovan, P. M.; Scott, L. T. *J. Am. Chem. Soc.* **2009**, *131*, 16006. (b) Bodwell, G. J. *Nat. Nanotechnol.* **2010**, *5*, 103. (c) Jasti, R.; Bertozzi, C. R. *Chem. Phys. Lett.* **2010**, *494*, 1. (d) Yu, X.; Zhang, J.; Choi, W. M.; Choi, J.-Y.; Kim, J. M.; Gan, L.; Liu, Z. *Nano Lett.* **2010**, *10*, 3343. (e) Fort, E. H.; Scott, L. T. *J. Mater. Chem.* **2011**, *21*, 1373. (f) Scott, L. T.; Jackson, E. A.; Zhang, Q.; Steinberg, B. D.; Bancu, M.; Li, B. *J. Am. Chem. Soc.* **2012**, *134*, 107.

(3) For reviews, see: (a) Omachi, H.; Segawa, Y.; Itami, K. *Acc. Chem. Res.* **2012**, *45*, 1378. (b) Hirst, E. S.; Jasti, R. *J. Org. Chem.* **2012**, *77*, 10473. (c) Yamago, S.; Kayahara, E.; Iwamoto, T. *Chem. Rec.* **2014**, *14*, 84.

(4) Jasti, R.; Bhattacharjee, J.; Neaton, J. B.; Bertozzi, C. R. *J. Am. Chem. Soc.* **2008**, *130*, 17646.

(5) (a) Takaba, H.; Omachi, H.; Yamamoto, Y.; Bouffard, J.; Itami, K. *Angew. Chem., Int. Ed.* **2009**, *48*, 6112. (b) Omachi, H.; Matsuura, S.; Segawa, Y.; Itami, K. *Angew. Chem., Int. Ed.* **2010**, *49*, 10202. (c) Segawa, Y.; Miyamoto, S.; Omachi, H.; Matsuura, S.; Sénel, P.; Sasamori, T.; Tokitoh, N.; Itami, K. *Angew. Chem., Int. Ed.* **2011**, *50*, 3244. (d) Segawa, Y.; Sénel, P.; Matsuura, S.; Omachi, H.; Itami, K. *Chem. Lett.* **2011**, *40*, 423. (e) Ishii, Y.; Nakanishi, Y.; Omachi, H.; Matsuura, S.; Matsui, K.; Shinohara, H.; Segawa, H.; Itami, K. *Chem. Sci.* **2012**, *3*, 2340. (f) Sibbel, F.; Matsui, K.; Segawa, Y.; Studer, A.; Itami, K. *Chem. Commun.* **2014**, *50*, 954.

(6) (a) Yamago, S.; Watanabe, Y.; Iwamoto, T. *Angew. Chem., Int. Ed.* **2010**, *49*, 757. (b) Iwamoto, T.; Watanabe, Y.; Sakamoto, Y.; Suzuki, T.; Yamago, S. *J. Am. Chem. Soc.* **2011**, *133*, 8354. (c) Kayahara, E.; Sakamoto, Y.; Suzuki, T.; Yamago, S. *Org. Lett.* **2012**, *14*, 3284. (d) Kayahara, E.; Iwamoto, T.; Suzuki, T.; Yamago, S. *Chem. Lett.* **2013**, *42*, 621. (e) Kayahara, K.; Patel, V. K.; Yamago, S. *J. Am. Chem. Soc.* **2014**, *136*, 2284.

(7) (a) Sisto, T. J.; Golder, M. R.; Hirst, E. S.; Jasti, R. *J. Am. Chem. Soc.* **2011**, *133*, 15800. (b) Xia, J.; Jasti, R. *Angew. Chem., Int. Ed.* **2012**, *51*, 2474. (c) Darzi, E. R.; Sisto, T. J.; Jasti, R. *J. Org. Chem.* **2012**, *77*, 6624. (d) Evans, P. J.; Darzi, E. R.; Jasti, R. *Nat. Chem.* **2014**, *6*, 404.

(8) (a) Sisto, T. J.; Tian, X.; Jasti, R. *J. Org. Chem.* **2012**, *77*, 5857. (b) Golder, M. R.; Wong, B. M.; Jasti, R. *J. Am. Chem. Soc.* **2012**, *134*, 19709.

(9) (a) Nishiuchi, T.; Feng, X.; Enkelmann, V.; Wagner, M.; Müllen, K. *Chem.—Eur. J.* **2012**, *18*, 16621. (b) Golling, F. E.; Quernheim, M.; Wagner, M.; Nishiuchi, T.; Müllen, K. *Angew. Chem., Int. Ed.* **2014**, *53*, 1525. (c) Tran-Van, A.-F.; Huxol, E.; Basler, J. M.; Neuburger, M.; Adjizian, J.-J.; Ewels, C. P.; Wegner, H. A. *Org. Lett.* **2014**, *16*, 1594. (d) Huang, C.; Huang, Y.; Akhmedov, N. G.; Popp, B. V.; Petersen, J. L.; Wang, K. K. *Org. Lett.* **2014**, *16*, 2672.

(10) Ishii, Y.; Matsuura, S.; Segawa, Y.; Itami, K. *Org. Lett.* **2014**, *16*, 2174.

(11) (a) Omachi, H.; Segawa, Y.; Itami, K. *Org. Lett.* **2011**, *13*, 2480. (b) Yagi, A.; Segawa, Y.; Itami, K. *J. Am. Chem. Soc.* **2012**, *134*, 2962. (c) Matsui, K.; Segawa, Y.; Itami, K. *Org. Lett.* **2012**, *14*, 1888. (d) Yagi, A.; Venkataramana, G.; Segawa, Y.; Itami, K. *Chem. Commun.* **2013**, *50*, 957.

(12) Iwamoto, T.; Kayahara, E.; Yasuda, N.; Suzuki, T.; Yamago, S. *Angew. Chem., Int. Ed.* **2014**, *53*, 6430.

(13) (a) Hitosugi, S.; Nakanishi, W.; Yamasaki, T.; Isobe, H. *Nat. Commun.* **2011**, *2*, 492. (b) Hitosugi, S.; Yamasaki, T.; Isobe, H. *J. Am. Chem. Soc.* **2012**, *134*, 12442. (c) Matsuno, T.; Kamata, S.; Hitosugi, S.; Isobe, H. *Chem. Sci.* **2013**, *4*, 3179.

(14) Omachi, H.; Nakamura, T.; Takahashi, E.; Segawa, Y.; Itami, K. *Nat. Chem.* **2013**, *5*, 572.

(15) (a) Segawa, Y.; Omachi, H.; Itami, K. *Org. Lett.* **2010**, *12*, 2262. (b) Segawa, Y.; Fukazawa, A.; Matsuura, S.; Omachi, H.; Yamaguchi, S.; Irle, S.; Itami, K. *Org. Biomol. Chem.* **2012**, *10*, 5979. (c) Nishihara, T.; Segawa, Y.; Itami, K.; Kanemitsu, Y. *J. Phys. Chem. Lett.* **2012**, *3*, 3125. (d) Fujitsuka, M.; Cho, D. W.; Iwamoto, T.; Yamago, S.; Majima, T. *Phys. Chem. Chem. Phys.* **2012**, *14*, 14585. (e) Camacho, C.; Niehaus, T. A.; Itami, K.; Irle, S. *Chem. Sci.* **2013**, *4*, 187. (f) Nishihara, T.; Segawa, Y.; Itami, K.; Kanemitsu, Y. *Chem. Sci.* **2014**, *5*, 2293.

(16) (a) Iwamoto, T.; Watanabe, Y.; Sadahiro, T.; Haino, T.; Yamago, S. *Angew. Chem., Int. Ed.* **2011**, *50*, 8342. (b) Xia, J.; Bacon, J. W.; Jasti, R. *Chem. Sci.* **2012**, *3*, 3018. (c) Iwamoto, T.; Watanabe, Y.; Takaya, H.; Haino, T.; Yasuda, N.; Yamago, S. *Chem.—Eur. J.* **2013**, *19*, 14061. (d) Nakanishi, Y.; Omachi, H.; Matsuura, S.; Miyata, Y.; Kitaura, R.; Segawa, Y.; Itami, K.; Shinohara, H. *Angew. Chem., Int. Ed.* **2014**, *53*, 3102. For CPP-related hosts, see: (e) Isobe, H.; Hitosugi, S.; Yamasaki, T.; Iizuka, R. *Chem. Sci.* **2013**, *4*, 1293. (f) Hitosugi, S.; Iizuka, R.; Yamasaki, T.; Zhang, R.; Murata, Y.; Isobe, H. *Org. Lett.* **2013**, *15*, 3199. (g) Sato, S.; Yamasaki, T.; Isobe, H. *Proc. Natl. Acad. Sci. U.S.A.* **2014**, *111*, 8374.

(17) Matsui, K.; Segawa, Y.; Namikawa, T.; Kamada, K.; Itami, K. *Chem. Sci.* **2013**, *4*, 84.

(18) (a) Seel, C.; Vögtle, F. *Angew. Chem., Int. Ed. Engl.* **1992**, *31*, 528. (b) Hof, F.; Craig, S. L.; Nuckolls, C.; Rebek, J. *Angew. Chem., Int. Ed.* **2002**, *41*, 1488.

(19) Kayahara, E.; Iwamoto, T.; Takaya, H.; Suzuki, T.; Fujitsuka, M.; Majima, T.; Yasuda, N.; Matsuyama, N.; Seki, S.; Yamago, S. *Nat. Commun.* **2013**, *4*, 2694.

(20) In the case of Yamago's cage (ref 19), the strain energy per carbon atom is 1.25 kcal·mol^{-1}, which is almost the same as that of [9]CPP (1.22 kcal·mol^{-1}).

(21) It was revealed that the blue-shift of the fluorescence spectra of CPPs is attributed to the increase of the HOMO−LUMO gap. See ref 15c.